Composites Science and Technology 181 (2019) 107689

Contents lists available at ScienceDirect

Composites Science and Technology

journal homepage: www.elsevier.com/locate/compscitech

Interfacially reinforced carbon fiber silicone resin via constructing functional nano-structural silver

Ying Li[a,1], Tong Zhang[a,1], Bo Jiang[a,**], Liwei Zhao[a], Hu Liu[b,c], Jiaoxia Zhang[b,d], Jincheng Fan[b,e], Zhanhu Guo[b,*], Yudong Huang[a,***]

[a] MIIT Key Laboratory of Critical Materials Technology for New Energy Conversion and Storage, School of Chemistry and Chemical Engineering, Harbin Institute of Technology, China

[b] Integrated Composites Laboratory (ICL), Department of Chemical & Biomolecular Engineering, University of Tennessee, Knoxville, TN, 37934, USA

[c] Key Laboratory of Materials Processing and Mold (Zhengzhou University), Ministry of Education, National Engineering Research Center for Advanced Polymer Processing Technology, Zhengzhou University, Zhengzhou, 450002, China

[d] School of Material Science and Engineering, Jiangsu University of Science and Technology, Zhenjiang, Jiangsu, 212003, China

[e] College of Materials Science and Engineering, Changsha University of Science and Technology, Changsha, 410114, China

ARTICLE INFO

Keywords:
Carbon fiber
Composite material
Interfacial property

ABSTRACT

The interfacial interaction between carbon fibers (CFs) and resin matrix is an important factor affecting mechanical performances of CF-based composites. In this work, a new approach combining electrodeposition method (EDM) and "Ag–S" bonds was applied to fabricate functional CF-based composites while preserving the mechanical properties of CFs. Silver nanoparticles were first attached on the CF surface by EDM. Then 4-aminothiophenol or 4-mercaptobenzoic acid was linked to Ag surface by Ag–S bonds to incorporate different functional groups onto the fiber surface. The interfacial shear strength was improved pronouncedly while the tensile strength was maintained consistent. The interfacial shear strength of the CFs after functionalized was increased 21.10% and 32.04%, respectively. However, the tensile strength of them decreased no more than 3%. With improved properties, these nanocomposites have potential applications for aerospace, transportation, electronics and other fields.

1. Introduction

Carbon fiber (CF) is an ideal reinforcement for polymer composites because of its excellent mechanical properties and light weight. Therefore, CF reinforced materials have been widely applied in aviation, military, and automotive industries [1–3]. The predominant properties of CF reinforced materials have a great relationship with the interfacial interaction between CF and the resin. However, chemically inert pristine CF presents low surface energy that leads to low interfacial bonding with the polymer matrix [4]. This property limits the real potential of CF, and could further affect the properties of the composite materials [5,6].

The CF surface modification has been extensively studied for enhancing the interfacial interactions between CF and polymer resin matrix. Those modifications mainly consist of wet chemical modification, dry chemical modification and multi-scale nanoparticle coating modification. Wet and dry chemical modifications [7,8] could promote the surface roughness and introduce the active functional groups on CF surface. However, those treatments could induce pits and flaws on the CF surface which led to crack initiation with an earlier and easier propagation [9,10]. Multi-scale methods such as chemical vapor deposition (CVD) could improve the roughness and the polarity of the CF surface [11,12]. But utilizing these methods could not effectively enhance the interfacial reactivity between CF and polymer resin matrix due to the absence of functional groups on the CF surface [13]. Though CVD can be used as efficiently multi-scale method [14,15], some issues including high temperature, toxic and expensive catalysts utilized in the CVD treatment restricted its applications.

Electrodeposition method (EDM) is a fast, simple, inexpensive and environmentally friendly method for preparing nanomaterials [16–18]. EDM could attach nanoparticles on the substrate with controllable morphology and size of nanoparticles (NPs) [19]. The NPs deposited by

* Corresponding author.
** Corresponding author.
*** Corresponding author.
E-mail addresses: jiangbo5981@hit.edu.cn (B. Jiang), zguo10@utk.edu (Z. Guo), huangyd@hit.edu.cn (Y. Huang).
[1] These authors contributed equally to this work.

https://doi.org/10.1016/j.compscitech.2019.107689
Received 10 October 2018; Received in revised form 21 May 2019; Accepted 14 June 2019
Available online 19 June 2019

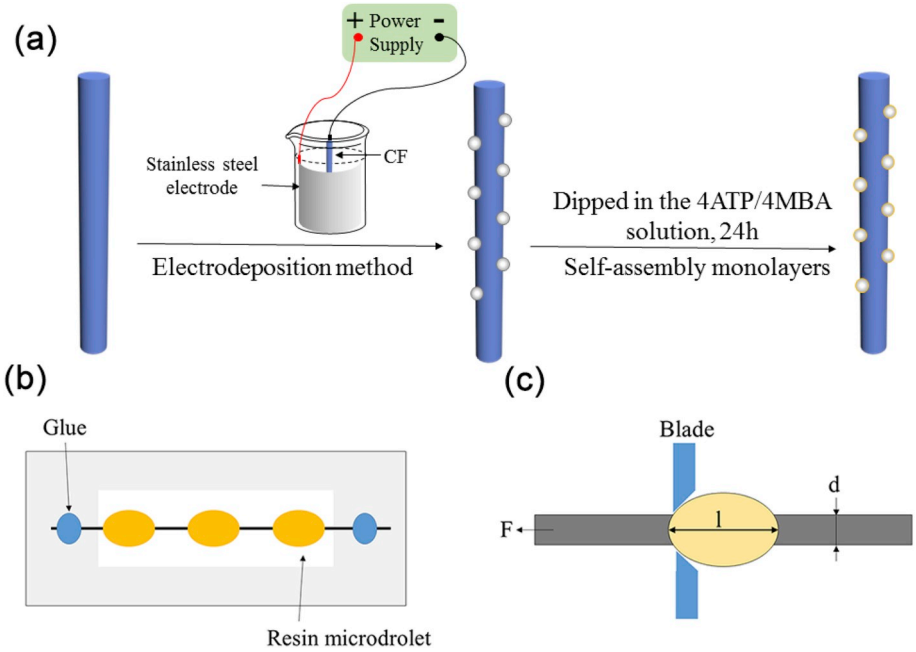

Fig. 1. Schematic sketches of the fabrication process of 4MBA-Ag@CF and 4ATP-Ag@CF (a), and the droplet test (b) and (c).

electrodeposition presented special properties, such as high specific surface area and high capacitive performances [20]. For noble metal NPs electrodeposition, only a small amount of noble salt could achieve the desired results [21,22]. Thiols link the active group to the silver or gold surfaces through a strong bond which is an effective way to introduce functional groups on the substrate [23]. This method endows the metal surface with new properties, such as hydrophilicity or hydrophobicity as well as other specific functionalities [24,25]. Therefore, combining EDM and "Ag–S″ bonds way provides a promising surface modification approach, which could overcome the deficiencies of the aforementioned methods.

In this paper, a novel strategy to functionalize CF surface by using EDM and "Ag–S″ bonds introduction is reported. Silver nanoparticles (Ag NPs) were coated uniformly on the CF surface by EDM, followed by introducing 4-mercaptobenzoic acid (4MBA) or 4-aminothiophenol (4ATP) via "Ag–S″ bonds to functionalize the Ag NP surface (Fig. 1a). The interfacial property and the mechanical property of functionalized CF were studied. The properties of CF composites modified by wet chemical methods were compared.

2. Experimental

2.1. Materials

Carbon fibers (T300 with 7 μm average diameter) used in this experiment were purchased from Toray Industries, Inc. 1-(3-dimethylaminopropyl)-3-ethylcarbodiimide hydrochloride (EDC), dimethylaminopyridine (DMAP), 2-Ethyl-4-methylimidazole, 4-Aminobenzenethiol (4ATP), 1,2-ethanediamine (EDA), 4-mercaptobenzoic acid (4MBA), $AgNO_3$, polyvinyl pyrrolidone, $NaNO_3$, sodium dodecylbenzenesulphonate, tetrahydrofuran (THF) and diiodomethane were supplied from Aladdin Industrial Corporation. γ-(2,3-Epoxypropoxy)propytrimethoxysilane (KH560) was purchased from Qufu Chenguang Chemical Co., Ltd. P.R. (China).

2.2. Preparation of Ag@CF

All the CF used in this experiment were refluxed in acetone at 70 °C for 48 h. As shown in the first step of Fig. 1a, the Ag@CF was prepared according to the previous procedures reported by Yin and co-workers [26]. The pristine CF was used as cathode and the stainless steel was used as anode. The electrolyte consisted of $AgNO_3$ (5 mM), sodium dodecylbenzenesulphonate (0.2 mM), PVP (1 mM), $NaNO_3$ (0.1 mM). The electrodeposition was carried out in the potentiostatic manner, 20 V at room temperature under ultra-sonication for 5 min.

2.3. Preparation of 4ATP-Ag@CF and 4MBA-Ag@CF

As illustrated in the second step of Fig. 1a, the Ag@CF was dipped in 10 mM (50 mL) 4ATP or 4MBA ethanol solution and stirred at room temperature for 24 h. Then the Ag@CF was rinsed with ethanol to remove the residues. Afterwards 4ATP-Ag@CF and 4MBA-Ag@CF were obtained after drying under vacuum for 24 h.

2.4. Preparation of silicone resin

The silicone resin was prepared by mixing 11.8 g KH560, 1.17 g deionized water and 2.3 g ethanol in one flask. The concentrated hydrochloric acid was added to adjust the pH of mixture to 4–5. Then the mixture was stirred at 55 °C for 4 h. The product was purified by vacuum-rotary evaporator for 40 min.

2.5. Characterization and technique

The morphology of the samples was investigated by Zeiss EVO18 with an acceleration voltage of 15 kV. The chemical composition and the surface elements of the CF were performed by X -ray photoelectron spectroscopy (XPS, ESCALAB 250Xi, ThermoFisher, USA). The Raman spectroscopy was recorded using a laser confocal Raman Microspectrometer (Renishaw, Gloucestershire, UK) with diode laser at 532 nm. The advancing contact angle of CF was performed on a dynamic contact angle analysis test (DCAT-21, Germany). Deionized water and diiodomethane were the test liquids as the polar solvent and the dispersive solvent, respectively. The single-fiber tensile testing machine (5569, Instron, USA) was used to assess the tensile strength of CF based on ASTMD3379-75. In order to evaluate the interfacial shear strength (IFSS) between CF and resin, the microdroplet (single fiber composite) test was operated by pulling a single CF out from cured resin droplets [27]. The schematic of microdroplet test is shown in Fig. 1b and c. The microdroplet samples were prepared by using silicone resin,

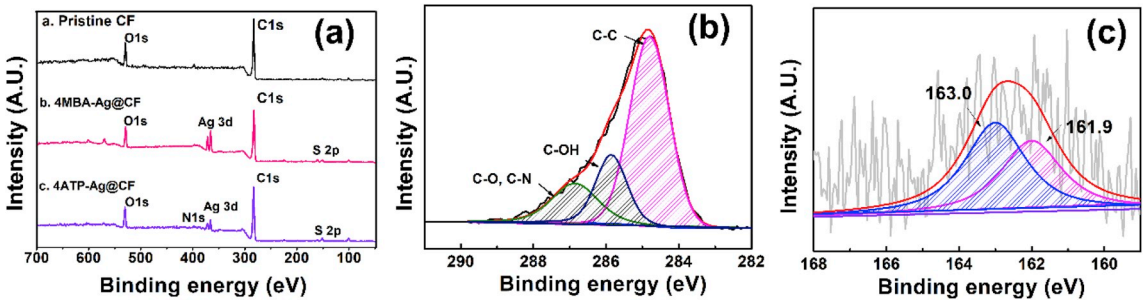

Fig. 2. XPS spectra of CF, 4MBA-Ag@CF and 4ATP-Ag@CF (a). High-resolution spectrum of C 1s (b) and S 2p (c) for 4ATP.

and 2-ethyl-4-methylimidazole as curing agent. They were mixed in a 100:32 mass ratio. The composites were cured for 2 h at 90, 120, 150 and 180 °C, respectively. The maximum load to pull out the CF from resin microdroplet was measured to calculate the IFSS values using the following equation:

$$\mathrm{IFSS} = \frac{F}{\pi dl} \quad (1)$$

where F is the maximum load recorded, d and l are the CF diameter and the embedded length, respectively.

3. Results and discussion

3.1. Surface chemical composition

XPS was used to investigate the chemical nature of carbon fiber with different treatments. The XPS spectra and the quantitative analysis are shown in Fig. 2a and Table S1. It was found that the surface composition of CF coated Ag NPs changed substantially. The elements on the pristine CF are C and O, as revealed in the XPS spectra. After treated by Ag NPs, the Ag 3d peaks were observed and the content of Ag atoms for Ag@CF, 4MBA-Ag@CF and 4ATP-Ag@CF was 1.89%, 2.1% and 1.06%, respectively. Fig. 2b presents the high-resolution XPS scan spectrum of C 1s for 4ATP-Ag@CF. The C 1s spectrum reveals the C–N peak at 285.9 eV because of the introduction of 4ATP [27], suggesting the successful grafting of 4ATP on the Ag@CF surface. The sulfur spectra of 4ATP-Ag@CF are fitted by S $2p_{3/2}$ and S $2p_{1/2}$ doublets at around 161.9 and 162.3 eV (Fig. 2c). The peak at 161.9 eV is attributed to the formation of a thiolate − Ag bond. The Ag 3d regions in the XPS data of Ag@CF show the Ag $3d_{5/2}$ and Ag $3d_{3/2}$ ionizations at 367.5 and 373.6 eV (Fig. S1a), which suggests that the majority of the silver atoms on the surfaces are the Ag (0) state [28]. On the contrary, 4MBA-Ag@CF shows Ag $3d_{5/2}$ and Ag $3d_{3/2}$ ionizations at 367.9 and 373.9 eV (Fig. S1b), respectively. Similarly, 4ATP bound Ag NPs show two peaks for Ag $3d_{5/2}$ and Ag $3d_{3/2}$ at 367.8 and 373.8 eV (Fig. S1c). The Ag $3d_{5/2}$ and $3d_{3/2}$ ionization energies of 4MBA-Ag@CF and 4ATP-Ag@CF are higher than Ag@CF. It indicates that outer Ag atoms bound with thiol. The XPS results further confirm the $–NH_2$ and –COOH were introduced via thiolate–Ag bond successfully.

Raman spectroscopy images effectively characterized the defects of CF as illustrated in Fig. 3. CF exhibits the D band at around 1369 cm^{-1} and the G band at 1589 cm^{-1}. The D band is assigned to the defects and disorder, and the G band is related to the C–C stretching on the graphitic structures of carbon. The intensity ratio I_D/I_G of D band and G band is related to the defective degree of CF surface [29]. Compared to the pristine CF, whose I_D/I_G ratio is 0.983, the ratios of CF-COOH and $CF-NH_2$ are significantly increased to 1.041 and 1.118, respectively. It indicates that the ratio of graphitic domains is decreased and the ratio of O or N elements is increased. Furthermore, the ratio I_D/I_G of 1.129 for the Ag@CF means that the Ag NPs should be covalently attached to the CF surface [30]. The Raman signal of the molecule on the rough Ag NPs surface could be magnified, which could obtain surface-enhanced Raman scattering (SERS). The Ag NPs based materials are usually used as SERS substrates [30–33]. Therefore, the SERS of the 4MBA-Ag@CF and the 4ATP-Ag@CF are shown in Fig. 3e–f. The S–H stretching band around 2500 cm^{-1} is not observed. However, the appearance of "Ag–S″ bonds stretching is observed at 225 and 222 cm^{-1} [33]. The results indicate that 4ATP or 4MBA is linked on Ag NPs surface successfully.

3.2. Surface morphology

The SEM images of pristine CF, CF-COOH, Ag@CF are shown in Fig. 4a–d, respectively. Significant differences of the surface morphology can be observed between the pristine CF and the CF-COOH. Shallow parallel grooves spread on the pristine fiber sparsely, along the longitudinal direction. After acidification, some grooves on the CF-COOH surface become more intensive and deeper. This means that nitric acid treatment produced defects on the CF surface.

As illustrated in Fig. 4c and d, electrodeposited Ag NPs on the CF surface are observed to be at a scale range from 26.67 to 180.61 nm (Fig. S2). The Ag NPs on the CF surface increased the surface roughness. The roughness plays a vital role in the improvement of interfacial adhesion. For 4MBA-Ag@CF and 4ATP-Ag@CF, their differences with Ag@CF cannot be recognized from SEM images as shown in Fig. S3.

3.3. Surface wettability

Differences in chemical environment and topography have a significant influence on surface energy. The improvement of the CF surface energy could increase the interface adhesion [34–36]. The advancing contact angle (θ), surface energy (γ), disperse part (γ^d), polar part (γ^P) of samples are shown in Table 1 and Table S2. As shown in Table S2, compared with the pristine CF, the CF-COOH and $CF-NH_2$ had 104.8% and 103.5% increase in the polar part, 7.1% and 5.4% increase in the dispersive part. The abundant oxygen functional groups within CF-COOH and amine groups within $CF-NH_2$ could contribute to the improvement in the polar part of the surface energy. Compared with the surface energy of the pristine CF, the value of Ag@CF is increased by 18.3% due to the improved roughness by Ag NPs. However, the results of 4MBA-Ag@CF and 4ATP-Ag@CF were enhanced 38.6% and 32.72%. This increased surface energy may be generated by the polar functional groups. Furthermore, the aromatic segment within the structure of the 4MBA-Ag@CF and 4ATP-Ag@CF plays a vital role in the surface energy of CF [24].

3.4. Tensile strength testing

The tensile strength (TS) of single fiber was investigated to reveal the effects of surface modification on the inherent mechanical properties of CFs. The TS of CF treated with different methods were compared. The tensile strength is decreased from 3.09 GPa for pristine CF to 2.63 GPa for CF-COOH (Fig. S4a). The tensile strength of $CF-NH_2$ is further decreased by 20.06%, compared with pristine CF. It could be caused by the defects on the treated CF. The results indicated that the

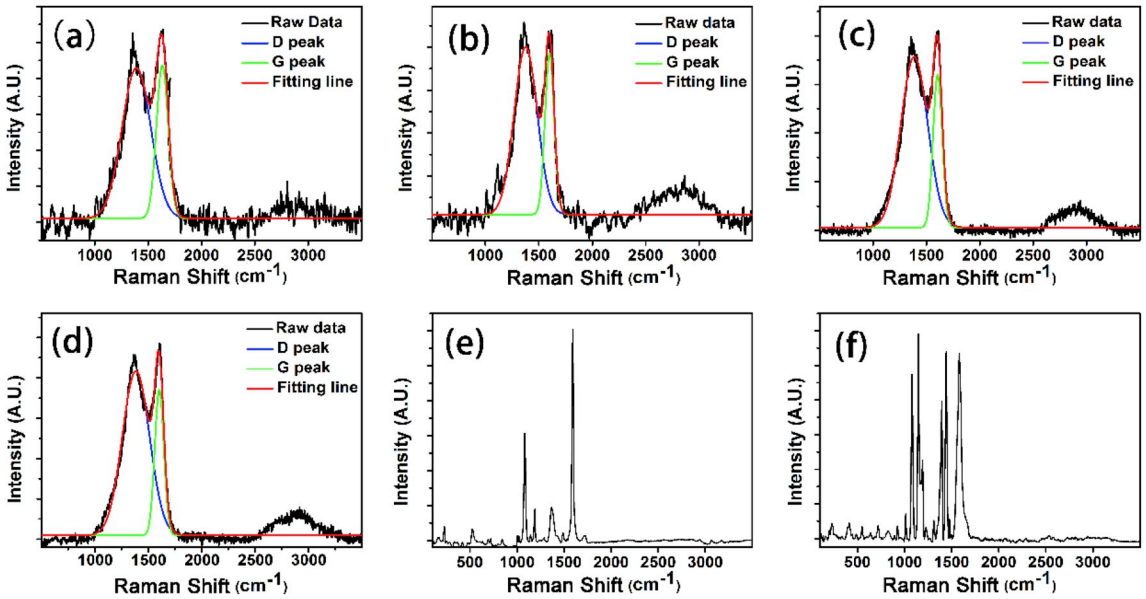

Fig. 3. Raman spectra of pristine CF (a), CF-COOH (b), CF-NH_2 (c), Ag@CF (d), SERS spectra of 4MBA-Ag@CF (e), 4ATP-Ag@CF (f).

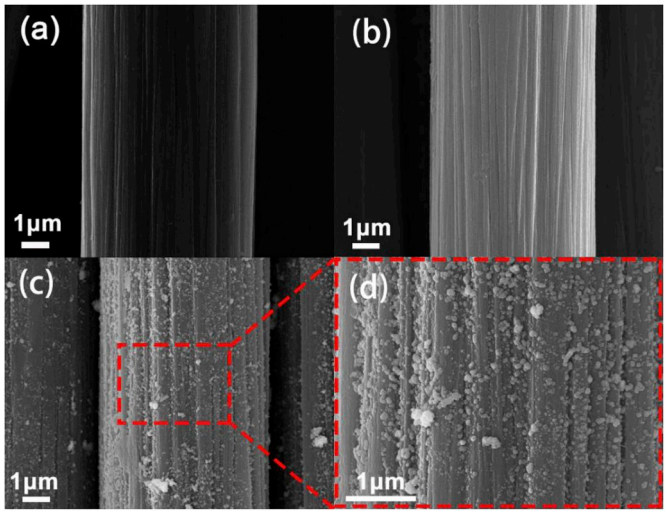

Fig. 4. SEM images of pristine CF (a), CF-COOH (b), Ag@CF (c) and (d).

Table 1
Surface energy of pristine CF, Ag@CF, 4MBA-Ag@CF and 4ATP-Ag@CF.

Fiber type	Contact angle (°)		Surface energy (mN/N)		
	θ_{water}	$\theta_{diiodomethane}$	γ^d	γ^p	γ
Pristine CF	75.80	62.33	32.28	6.93	39.21
Ag@CF	61.01	49.85	34.23	12.15	46.38
4MBA-Ag@CF	56.76	45.19	37.67	16.66	54.33
4ATP-Ag@CF	59.29	47.25	36.83	15.21	52.04

acidification and amination treatment has a negative effect on the carbon fiber property. As Fig. 5a reveals, the tensile strength values of Ag@CF, 4MBA-Ag@CF and 4ATP-Ag@CF were 2.99, 3.04 and 3.01 GPa, respectively. Compared to pristine CF, the values of 4MBA-Ag@CF and 4ATP-Ag@CF showed negligible decreases of 1.61% and 2.59%, respectively. The results of tensile strength testing imply that different functional treatments have obvious influences on the CF mechanical properties. The defects introduced by acidic etching reduced the tensile strength [1,7]. However, the mechanical property of CF treated with EDM and "Ag–S" bonds was almost not affected.

3.5. Interfacial property of CF composites

The interfacial properties have a major effect on the mechanical properties of the final composites. The interfacial bonding strength between the matrix and the studied fibers was evaluated by the IFSS, and the IFSS results are shown in Fig. 5b and Fig. S4b. The IFSS results of pristine CF, CF-COOH, CF-NH_2, Ag@CF, 4MBA-Ag@CF and 4ATP-Ag@CF are 34.36, 37.71, 39.81, 41.49, 41.61 and 45.37 MPa, respectively. Compared with the pristine CF, the IFSS of CF-COOH and CF-NH_2 are increased by 9.75% and 15.86%, respectively. However, as expected, the IFSS of 4MBA-Ag@CF and 4ATP-Ag@CF exhibit greater enhancement of 21.10% and 32.04%, respectively. The increment for IFSS value is superior to the CFs functionalized by chemical plating, which was only 22.9% [33]. On one hand, the Ag NPs deposited by EDM are uniform at the nanoscale. The attachment of Ag NPs improves the surface energy as the mentioned above and thus leads to a better adhesion with resin matrix via the mechanical interlocking [37]. On the other hand, the epoxy moieties of the resin substrate could react with amine [31]. The IFSS results reveal that the interfiacial property of 4ATP-Ag@CF is higher than the others. The incorporation of 4ATP on the CF surface could provide an amino which act as reactive anchoring site for the epoxy group of silicone resin matrix, shown in Fig. 5c. It's suggesting that the improvement of interfacial property is caused by the combination of Ag NPs and amino group. When the resin matrix of the CF composite was instead by epoxy resin, the same result were obtained as shown in Fig. S5. Therefore, this combined EDM and "Ag–S" bonds treatments can guarantee to increase the interfacial property of CF composite which the resin matrix contain epoxy group.

The CF surface morphologies after IFSS experiments were observed (Fig. 6a–d). For the pristine CF, minimal resin fragment remained on the surface after debonding. It means that the microdroplets were debonded smoothly due to the weak van der Waals force reaction between CF and resin matrix (Fig. 6a). The limited number of bonds between CF surface and resin matrix leads to a weak adhesion of pristine CF composite (Fig. 6e). For CF-COOH and CF-NH_2, there is few resin remaining on the fiber surface, indicating poor interfacial properties with silicone resin (Fig. S6). However, for 4ATP-Ag@CF, the resin fragment on the surface can be observed clearly (Fig. 6d). The Ag NPs, which can be observed obviously on the CF surface, contributed to modulus gradient diffusing between the CF and low modulus silicone resin matrix, thus resulting in a decline in the localized stress concentrations. The treatment of CF with Ag NPs covered with amino group can provide further

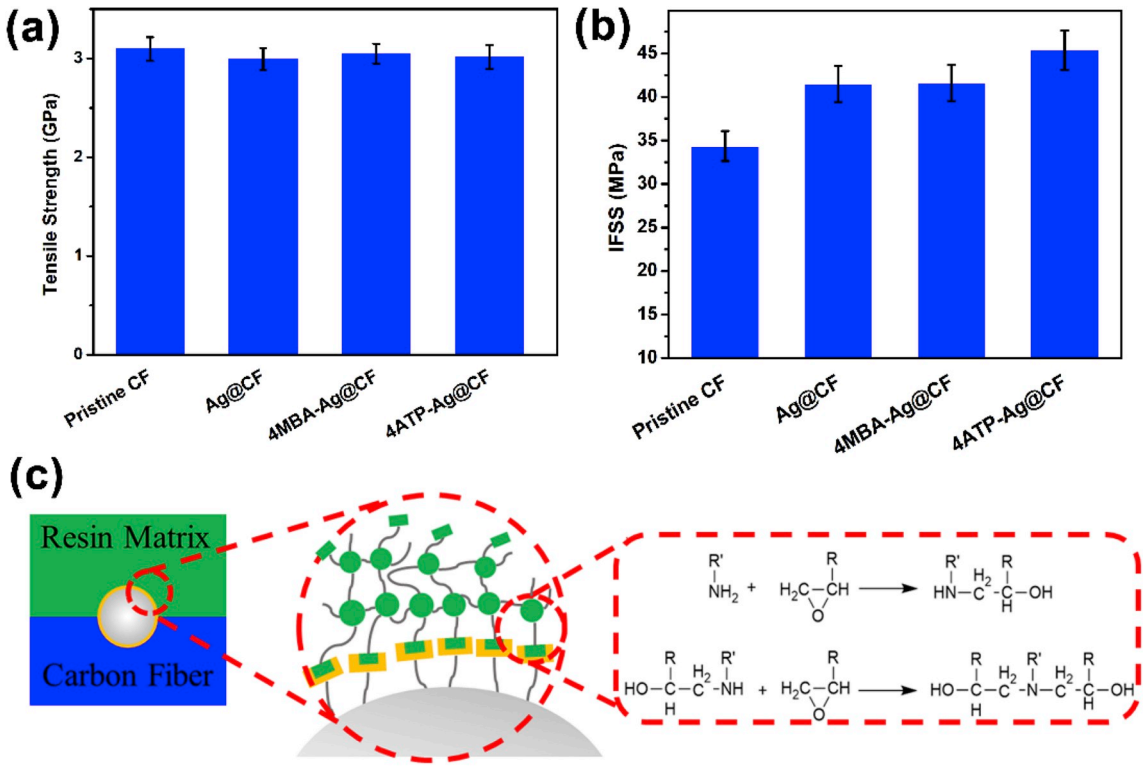

Fig. 5. (a)Tensile strength, (b) interfacial shear strength (IFSS) results of pristine CF, Ag@CF, 4MBA-Ag@CF and 4ATP-Ag@CF, (c) diagram of chemical bonding in the interface.

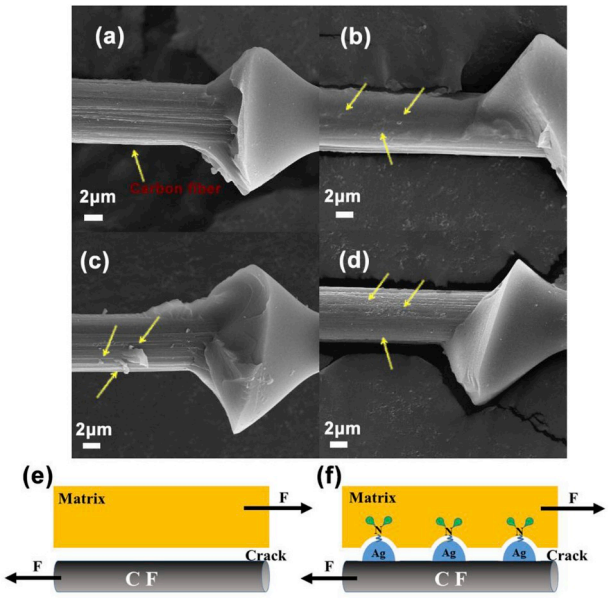

Fig. 6. SEM images of pristine CF (a), Ag@CF (b), 4MBA-Ag@CF (c), 4ATP-Ag@CF (d) and schematics of fiber-epoxy junction failure mechanism (e, f).

interfacial interaction, with not only van der Waals force but also chemical bonding. As shown in Fig. 6f, the amino group from CF surface could react with the epoxy groups of silicone resin, thus improved the interfacial adhesion of 4ATP-Ag@CF composite [38]. Therefore, as the arrow pointed, the remained residued silicone resin fragments which remaining on the 4ATP-Ag@CF surface indicates that stronger interfacial shear strength was formed.

4. Conclusions

In summary, Ag NPs and 4ATP were successfully formed on the CF surface by a novel approach which consists of EDM and "Ag–S" bonds. These results demonstrate that the IFSS of 4ATP-Ag@CF and 4ATP-Ag@CF composites were 21.10% and 32.04% higher than pristine CF composites, which was caused by the formation of mechanical interlock through chemical bonding. EDM and "Ag–S" bond treatments not only maintained the mechanical properties of CF, but also enhanced the interfacial performance of CF significantly. Combination of EDM and "Ag–S" bonds is not only convenient to apply but also highly effective to improve the interfacial properties of CF and resin matrix.

Acknowledgement

This work was financially supported by the National Natural Science Foundation of China (Grant No. 51673054), the Harbin City Science and Technology Innovation Talent Foundation (Grant No. 2017RAYXJ003), Shanghai Space Science and Technology Innovation Foundation (Grant No. SAST2017-114), the Fundamental Research Funds for the Central Universities, China (Grant No.222201717001).

Appendix A. Supplementary data

Supplementary data to this article can be found online at https://doi.org/10.1016/j.compscitech.2019.107689.

References

[1] J.M. Yuan, Z.F. Fan, Q.C. Yang, W. Li, Z.J. Wu, Surface modification of carbon fibers by microwave etching for epoxy resin composite, Compos. Sci. Technol. 164 (2018) 222–228.
[2] J. Yu, L. Meng, D. Fan, C. Zhang, F. Yu, Y. Huang, The oxidation of carbon fibers through $K_2S_2O_8$/$AgNO_3$ system that preserves fiber tensile strength, Composites, Part B 60 (2014) 261–267.
[3] C. Deng, J. Jiang, F. Liu, L. Fang, J. Wang, D. Li, J. Wu, Influence of carbon

nanotubes coatings onto carbon fiber by oxidative treatments combined with electrophoretic deposition on interfacial properties of carbon fiber composite, Appl. Surf. Sci. 357 (2015) 1274–1280.
[4] B.J. Kim, S.H. Cha, K. Kong, W. Ji, H.W. Park, Y.B. Park, Synergistic interfacial reinforcement of carbon fiber/polyamide 6 composites using carbon nanotube modified silane coating on ZnO nanorod grown carbon fiber, Compos. Sci. Technol. 165 (2018) 362–372.
[5] A.R. Jones, A. Cintora, S.R. White, N.R. Sottos, Autonomic healing of carbon fiber/epoxy interfaces, ACS Appl. Mater. Interfaces 6 (9) (2014) 6033–6039.
[6] X. Liu, X. Yin, L. Kong, Q. Li, Y. Liu, W. Duan, L. Zhang, L. Cheng, Fabrication and electromagnetic interference shielding effectiveness of carbon nanotube reinforced carbon fiber/pyrolytic carbon composites, Carbon 68 (2014) 501–510.
[7] M. Sharma, S. Gao, E. Mäder, H. Sharma, L.Y. Wei, J. Bijwe, Carbon fiber surfaces and composite interphases, Compos. Sci. Technol. 102 (2014) 35–50.
[8] M.A. Montes Morán, F.W.J. van Hattum, J.P. Nunes, A. Martínez-Alonso, J.M.D. Tascón, C.A. Bernardo, A study of the effect of plasma treatment on the interfacial properties of carbon fibre thermoplastic composites, Carbon 43 (8) (2005) 1795–1799.
[9] B. Demir, L.C. Henderson, T.R. Walsh, Design rules for enhanced interfacial shear response in functionalized carbon fiber epoxy composites, ACS Appl. Mater. Interfaces 9 (13) (2017) 11846–11857.
[10] B. Jiang, T. Zhang, L. Zhao, Y. Huang, Interfacially reinforced carbon fiber composites by grafting modified methylsilicone resin, Compos. Sci. Technol. 140 (2017) 39–45.
[11] Y.N. Liu, M. Li, Y. Gu, X. Zhang, J. Zhao, Q. Li, Z. Zhang, The interfacial strength and fracture characteristics of ethanol and polymer modified carbon nanotube fibers in their epoxy composites, Carbon 52 (2013) 550–558.
[12] Q. Liu, M. Li, Y. Gu, S. Wang, Y. Zhang, Q. Li, L. Gao, Z. Zhang, Interlocked CNT networks with high damping and storage modulus, Carbon 86 (2015) 46–53.
[13] O. Zabihi, M. Ahmadi, Q. Li, S. Shafei, M.G. Huson, M. Naebe, Carbon fibre surface modification using functionalized nanoclay: a hierarchical interphase for fibre-reinforced polymer composites, Compos. Sci. Technol. 148 (2017) 49–58.
[14] R. Li, N. Lachman, P. Florin, H.D. Wagner, B.L. Wardle, Hierarchical carbon nanotube carbon fiber unidirectional composites with preserved tensile and interfacial properties, Compos. Sci. Technol. 117 (2015) 139–145.
[15] J. Dong, C. Jia, M. Wang, X. Fang, H. Wei, H. Xie, T. Zhang, J. He, Z. Jiang, Y. Huang, Improved mechanical properties of carbon fiber-reinforced epoxy composites by growing carbon black on carbon fiber surface, Compos. Sci. Technol. 149 (2017) 75–80.
[16] F. Movassagh-Alanagh, A. Bordbar-Khiabani, A. Ahangari-Asl, Three-phase PANI@nano-Fe_3O_4@CFs heterostructure: fabrication, characterization and investigation of microwave absorption and EMI shielding of PANI@nano-Fe_3O_4 @CFs/epoxy hybrid composite, Compos. Sci. Technol. 150 (2017) 65–78.
[17] P. Kainourgios, I.A. Kartsonakis, D.A. Dragatogiannis, E.P. Koumoulos, P. Goulis, C.A. Charitidis, Electrochemical surface functionalization of carbon fibers for chemical affinity improvement with epoxy resins, Appl. Surf. Sci. 416 (2017) 593–604.
[18] C. Li, M. Iqbal, J. Lin, X. Luo, B. Jiang, V. Malgras, K.C. Wu, J. Kim, Y. Yamauchi, Electrochemical deposition: an advanced approach for templated synthesis of nanoporous metal architectures, Acc. Chem. Res. 51 (2018) 1764–1773.
[19] C. Wang, J. Li, S. Sun, X. Li, G. Wu, Y. Wang, F. Xie, Y. Huang, Controlled growth of silver nanoparticles on carbon fibers for reinforcement of both tensile and interfacial strength, RSC Adv. 6 (17) (2016) 14016–14026.
[20] Y. Yan, B. Li, W. Guo, H. Pang, H. Xue, Vanadium based materials as electrode materials for high performance supercapacitors, J. Power Sources 329 (2016) 148–169.
[21] Q. Hong, H. Lu, In-situ electrodeposition of highly active silver catalyst on carbon fiber papers as binder free cathodes for aluminum-air battery, Sci. Rep. 7 (1) (2017) 3378.
[22] R. Liu, K. Ye, Y. Gao, W. Zhang, G. Wang, D. Cao, Ag supported on carbon fiber cloth as the catalyst for hydrazine oxidation in alkaline medium, Electrochim. Acta 186 (2015) 239–244.
[23] S. Herrera, F. Tasca, F.J. Williams, E.J. Calvo, P. Carro, R.C. Salvarezza, Surface structure of 4-mercaptopyridine on Au(111): a new dense phase, Langmuir 33 (38) (2017) 9565–9572.
[24] C. Vericat, M.E. Vela, G. Benitez, P. Carro, R.C. Salvarezza, Self-assembled monolayers of thiols and dithiols on gold: new challenges for a well-known system, Chem. Soc. Rev. 39 (5) (2010) 1805.
[25] B. Cao, Y. Peng, X. Liu, J. Ding, Effects of functional groups of materials on nonspecific adhesion and chondrogenic induction of mesenchymal stem cells on free and micropatterned surfaces, ACS Appl. Mater. Interfaces 9 (28) (2017) 23574–23585.
[26] B. Yin, H. Ma, S. Wang, S. Chen, Electrochemical Synthesis of silver nanoparticles under protection of poly(N-vinylpyrrolidone), J. Phys. Chem. B 107 (34) (2003) 8898–8904.
[27] F. Ran, Y. Wu, M. Jiang, Y. Tan, Y. Liu, L. Kong, L. Kang, S. Chen, Nanocomposites based on hierarchical porous carbon fiber@vanadium nitride nanoparticles as supercapacitor electrodes, Dalton Trans. 47 (12) (2018) 4128–4138.
[28] S. Bandyopadhyay, S. Chattopadhyay, A. Dey, Protonation state of thiols in self-assembled monolayers on roughened Ag/Au surfaces and nanoparticles, Phys. Chem. Chem. Phys. 17 (38) (2015) 24866–24873.
[29] Y. Liu, C. Hou, T. Jiao, J. Song, X. Zhang, R. Xing, J. Zhou, L. Zhang, Q. Peng, Self-Assembled AgNP-containing nanocomposites constructed by electrospinning as efficient dye photocatalyst materials for wastewater treatment, Nanomaterials 8 (1) (2018).
[30] E.S. Orth, J.E.S. Fonsaca, S.H. Domingues, H. Mehl, M.M. Oliveira, A.J.G. Zarbin, Targeted thiolation of graphene oxide and its utilization as precursor for graphene/silver nanoparticles composites, Carbon 61 (2013) 543–550.
[31] P. Liou, F.X. Nayigiziki, F. Kong, A. Mustapha, M. Lin, Cellulose nanofibers coated with silver nanoparticles as a SERS platform for detection of pesticides in apples, Carbohydr. Polym. 157 (2017) 643–650.
[32] W. Lai, J. Zhou, Y. Liu, Z. Jia, S. Xie, L. Petti, P. Mormile, 4MBA-labeled Ag-nanorod aggregates coated with SiO_2: synthesis, SERS activity, and biosensing applications, Anal. Methods 7 (20) (2015) 8832–8838.
[33] J. He, Y. Huang, L. Meng, H. Cao, H. Gu, Effects of chain lengths, molecular orientation, and functional groups of thiols adsorbed onto CF surface on interfacial properties of CF/epoxy composites, J. Appl. Polym. Sci. 112 (6) (2009) 3380–3387.
[34] M. Ahmadi, O. Zabihi, M. Masoomi, M. Naebe, Synergistic effect of MWCNTs functionalization on interfacial and mechanical properties of multi-scale UHMWPE fibre reinforced epoxy composites, Compos. Sci. Technol. 134 (2016) 1–11.
[35] B. Song, T. Wang, L. Wang, H. Liu, X. Mai, X. Wang, N. Wang, Y. Huang, Y. Ma, Y. Lu, E.K. Wujcik, Z. Guo, Interfacially reinforced carbon fiber/epoxy composite laminates via in-situ synthesized graphitic carbon nitride (g-C_3N_4), Compos. Sci. Technol. 158 (2019) 259–268.
[36] J.M. Yuan, Z.F. Fan, Q.C. Yang, W. Li, Z.J. Wu, Surface modification of carbon fibers by microwave etching for epoxy resin composite, Compos. Sci. Technol. 164 (2018) 222–228.
[37] B. Song, T. Wang, H. Sun, H. Liu, X. Mai, X. Wang, L. Wang, N. Wang, Y. Huang, Z. Guo, Graphitic carbon nitride (g-C_3N_4) interfacially strengthened carbon fiber epoxy composites, Compos. Sci. Technol. 167 (2018) 515–521.
[38] Q. Wu, R. Zhao, Q. Liu, T. Jiao, J. Zhu, F. Wang, Simultaneous improvement of interfacial strength and toughness between carbon fiber and epoxy by introducing amino functionalized ZrO_2 on fiber surface, Mater. Des. 149 (2018) 15–24.